

RADIATION AND MAGNETOHYDRODYNAMIC EFFECTS ON CONVECTIVE NANOFLUID PAST AN INCLINED PLATE IN THE PRESENCE OF A CHEMICAL REACTION

G. PALANI*

Department of Mathematics
Dr Ambedkar Govt Arts College, Chennai 600039, Tamil Nadu, INDIA
E-mail: gpalani32@yahoo.co.in

A. ARUTCHELVI

Department of Mathematics
Bharathi Women's College, Chennai 600108, Tamil Nadu, INDIA

This computational work explores the heat and mass transfer of copper water nanofluid flowing along an inclined plate with varying surface temperature and concentration in the presence of a magnetic field and radiation through a permeable medium. The dimensionless governing equations are solved numerically using an efficient finite-difference technique, which is fast convergent and unconditionally stable. The findings are reviewed and illustrated through graphs for pertinent parameters.

Key words: finite difference, nanofluids, viscous dissipation, heat source, porous medium.

1. Introduction

Nanoparticle study is currently a hot area for several researchers. Due to an innovative technique for increasing thermal conductivity, nanofluids have seen widespread use in engineering and medicine over the last few decades. Specifically convective heat transfer in nanofluids plays a significant role in engineering processes, such as heating or cooling technique of electronic components, highly developed nuclear systems, solar collector, thermal isolation systems, food processes, etc. Countless biomedical applications necessitate nanofluids, for example in, magnetic cell division, drug delivery, cancer therapeutics, nano-cryosurgery, etc.

Chien-Hsin Chen [1] studied MHD flow with Ohmic heating and viscous dissipation impact on a vertical surface and found that when viscous dissipation increases, the rate of heat transfer decreases. Rising Schmidt numbers or buoyancy ratio tend to raise the local Sherwood number and slow down the local skin friction. Palani and Kim [2] looked into the effect of viscous dissipation over a semi-infinite plate on a free convective flow with a changing temperature. They discovered that the velocity reaches a steady-state by raising the value of the Prandtl number and local skin friction rises for higher values of viscous dissipation, but a reverse effect is observed in the case of average Nusselt number. Vasu, Prasad, and Reddy [3] analyzed the transient free convective radiating flow past a vertical plate with thermal flux and noticed that velocity and temperature increase as radiation parameters decrease. Subhas Abel *et al.* [4] explored an MHD laminar flow over an upright permeable stretching sheet with the effects of buoyancy and viscous dissipation; and noticed that the influence of the suction parameter decreased and the injection parameter increased the longitudinal velocity. RamReddy *et al.* [5] analysed the impact of viscous dissipation and magnetic field on a free convective flow in a permeable medium and came up with the result that an increment in the viscous dissipation factor leads to increased velocity and temperature fields. Ganesan, Suganthi and Loganathan [6] discussed the

* To whom correspondence should be addressed

Ohmic heating effect in a doubly stratified natural convective flow over an upright plate. They found that the concentration enhances once the thermal stratification increases, and the temperature declines as the mass stratification increases. Srikanth, Srinivas, and Reddy [7] discussed the consequence of the heat source parameter on a magnetohydrodynamic nanofluid flow past a porous inclined plate. They noticed that an increment in the angle of inclination raises the thermal boundary layer.

Dulal Pal and Gopinath Mandal [8] considered a mixed MHD flow past an extended sheet in a porous medium with the effects of viscous dissipation and heat source. Their investigation demonstrated that an increment in the nanofluid volume fraction enhances skin friction. Temperature profile raises with rising values of heat generation parameter. Hemalatha *et al.* [9] discussed the impact of the magnetic field, viscous dissipation and radiation over a stretching sheet. They inferred that heat transfer of Al_2O_3 and TiO_2 -water nanofluid exhibits smaller changes when compared to Cu-water nanofluid. Meraj Mustafa *et al.* [10] explored the impact of electromagnetic field on free convective nanofluid flow over an upright plate. They concluded that an increment in the Brownian motion or thermophoretic increases temperature distribution. Mohsen Sheikholes *et al.* [11] analyzed the effect of viscous dissipation and an MHD nanofluid flow over two horizontal parallel plates in a rotating system. They noticed that with increasing the nanoparticle volume fraction, the Nusselt number increases but it decreases with increasing the Eckert number and magnetic parameter. Gangaa *et al.* [12] discussed an MHD unsteady natural convective flow over an upright plate with Ohmic and viscous dissipation and noticed that when there is viscous dissipation, the nanofluid velocity increases and at the same time velocity decreases for increasing values of the magnetic parameter. Bhaskar Reddy *et al.* [13] examined the impact of viscous dissipative heat and chemical reactions on a natural convection flow over a moving plate in a permeable medium. It was concluded that an increment in the volume fraction or Biot number slows down the velocity of Cu-nanoparticle, and at the same time velocity increases for higher values of the Eckert number. Loganathan and Sivapoornapriya [14] investigated the consequence of Ohmic heat and viscous dissipative parameter past over a vertical plate in a permeable medium and concluded that an increment in viscous dissipation or Ohmic heating increases velocity but decelerates the temperature profile. Veeresh *et al.* [15] explored the transfer of heat in a mixed convective flow in a permeable moving plate. It was observed that temperature increases as the radiation or heat source parameter decline. An increment in the angle of inclination or Schmidt number diminishes the velocity whereas it increases for the Grashof number or permeability parameter.

Kumaresan *et al.* [16] discussed the free convective chemically reacting flow of a silver fluid past a vertical plate in a permeable medium. They observed that velocity and temperature decrease and increase respectively as the radiation parameters increases. Prakash *et al.* [17] reviewed the effects of viscous and Ohmic heating taken together on an inclined nonlinear stretching sheet surrounded by a permeable medium and observed that the effect of the suction factor reduces both temperature and the skin friction coefficient. Sidda Reddy, Chandra Reddy and Raju [18] studied the influence of thermal diffusion and Joule heating on MHD free convective flow surrounded in a porous medium, they found that the growing values of Soret number increase concentration profile and decrease skin friction coefficient. Srinivasa and Ajay [19] examined the internal heat absorption and viscous dissipative heat in a free convection flow under an applied magnetic field on a vertical flat plate. They observed that an increment in the viscous dissipative term or internal heat generation increases velocity and temperature profiles.

The above studies motivated to investigate the effects of viscous dissipation on an unsteady free convective MHD radiating copper water nanofluid flow over an inclined plate in a permeable medium in the presence of variable surface temperature and concentration.

2. Mathematical analysis

Consider an unsteady free convective flow of an incompressible nanofluid over a semi-infinite plate inclined at an angle α vertically in a permeable medium with the effects of radiation, viscous dissipation, and heat source with varying surface concentration and temperature. Here, the co-ordinate axes are taken along and normal to the plate. Let T'_w and C'_w be the temperature and concentration near the plate and the fluid initially at a time $t = 0$. At time $t > 0$, the temperature as well as the concentration near the plate rise to T'_∞

and C'_∞ , respectively. The electromagnetic field is applied perpendicular to the fluid flow direction in this instance. The entire properties of a fluid are supposed to be invariable, excluding the body force. The schematic diagram and Cartesian coordinate system of the problem are shown in Fig.1.

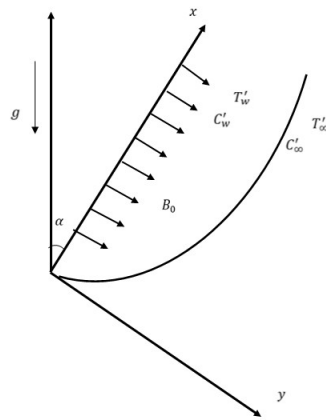


Fig.1. The physical model and coordinate system.

The nanofluid used for this study is water mixed with copper nanoparticles. As Cu nanoparticles and water are in thermal equilibrium, no slip condition occurs. Considering the aforementioned assumptions, the resulting equations are

$$\frac{\partial u}{\partial x} + \frac{\partial v}{\partial y} = 0, \tag{2.1}$$

$$\rho_{nf} \left(\frac{\partial u}{\partial t'} + u \frac{\partial u}{\partial x} + v \frac{\partial u}{\partial y} \right) = \mu_{nf} \frac{\partial^2 u}{\partial y^2} + g(\rho\beta_T)_{nf} (T' - T'_\infty) \cos \alpha + g(\rho\beta_C)_{nf} (C' - C'_\infty) \cos \alpha - \sigma_{nf} B_0^2 u - \frac{\mu_f}{k'_p} u, \tag{2.2}$$

$$(\rho c_p)_{nf} \left(\frac{\partial T'}{\partial t'} + u \frac{\partial T'}{\partial x} + v \frac{\partial T'}{\partial y} \right) = k_{nf} \frac{\partial^2 T'}{\partial y^2} - \frac{\partial q_r}{\partial y} + Q_0 (T' - T'_\infty) + \sigma_{nf} B_0^2 u^2 + \mu_{nf} \left(\frac{\partial u}{\partial y} \right)^2, \tag{2.3}$$

$$\left(\frac{\partial C'}{\partial t'} + u \frac{\partial C'}{\partial x} + v \frac{\partial C'}{\partial y} \right) = D \frac{\partial^2 C'}{\partial y^2} - k'_c (C' - C'_\infty). \tag{2.4}$$

Related boundary conditions are

$$\begin{aligned} t' \leq 0: \quad & u = 0, \quad v = 0, \quad T' = T'_\infty, \quad C' = C'_\infty \quad \text{for all } x, y, \\ t' > 0: \quad & u = 0, \quad v = 0, \quad T' = ax^n + T'_\infty, \quad C' = bx^m + C'_\infty \quad \text{as } y = 0, \\ & u \rightarrow 0, \quad T' \rightarrow T'_\infty, \quad C' \rightarrow C'_\infty \quad \text{as } y \rightarrow \infty. \end{aligned} \tag{2.5}$$

Table 1. Thermophysical properties of water and Cu nanoparticle.

| Physical properties | ρ (kg / m ³) | C_p (J / gK) | k (W / mK) | $\beta \times 10^5$ (K ⁻¹) | σ (S / m) |
|---------------------|-------------------------------|----------------|--------------|--|-----------------------|
| Water | 997.1 | 4179 | 0.613 | 21 | 5.5×10^{-6} |
| Cu | 8933 | 385 | 401 | 1.67 | 59.6×10^{-6} |

Radiation is reduced into

$$q_r = \frac{-4\sigma}{3K^*} \frac{\partial T'^4}{\partial y}, \quad \frac{\partial q_r}{\partial y} = -4a^* \sigma (T_\infty'^4 - T^4), \quad T'^4 \cong 4T_\infty'^3 T' - 3T_\infty'^4. \quad (2.6)$$

Equation (2.3) is reduced using Eq.(2.6)

$$\begin{aligned} (\rho c_p)_{nf} \left(\frac{\partial T'}{\partial t'} + u \frac{\partial T'}{\partial x} + v \frac{\partial T'}{\partial y} \right) = \\ = k_{nf} \frac{\partial^2 T'}{\partial y^2} + 16a^* \sigma T_\infty'^3 T (T'_w - T'_\infty) + Q_0 (T' - T'_\infty) + \sigma_{nf} B_0^2 u^2 + \mu_{nf} \left(\frac{\partial u}{\partial y} \right)^2. \end{aligned} \quad (2.7)$$

Non-dimensional quantites are

$$\begin{aligned} X = \frac{x}{L}, \quad Y = \frac{y}{L} Gr_L^{1/4}, \quad U = \frac{uL}{\nu_f} Gr_L^{-1/2}, \quad V = \frac{vL}{\nu_f} Gr_L^{-1/4}, \quad t = \frac{t' \nu_f}{L^2} Gr_L^{1/2}, \\ T = \frac{T' - T'_\infty}{T'_w(L) - T'_\infty}, \quad C = \frac{C' - C'_\infty}{C'_w - C'_\infty}, \quad k_p^2 = \frac{L^2}{K'_p} Gr_L^{-1/2}, \quad k_c = \frac{k'_c L^2}{\nu_f} Gr_L^{-1/2}, \quad Pr = \frac{(\mu c_p)_f}{k_f}, \\ M = \frac{B_0^2 \sigma_f L^2}{\rho_f \nu_f} Gr_L^{-1/2}, \quad Sc = \frac{\nu}{D}, \quad R = \frac{16a^* \sigma T_\infty'^3 L^2}{k_f} Gr_L^{-1/2}, \quad Q = \frac{Q_0 L^2}{\nu_f (\rho c_p)_f} Gr_L^{-1/2} \end{aligned} \quad (2.8)$$

where

$$\begin{aligned} \rho_{nf} = (1 - \phi) \rho_f + \phi \rho_s, \quad \mu_{nf} = \frac{\mu_f}{(1 - \phi)^{2.5}}, \\ \sigma_{nf} = \sigma_f \left[1 + \frac{3(\sigma - 1)\phi}{(\sigma + 2) - (\sigma - 1)\phi} \right], \quad k_{nf} = k_f \left[\frac{k_s + 2k_f - 2\phi(k_f - k_s)}{k_s + 2k_f + \phi(k_f - k_s)} \right], \\ (\rho c_p)_{nf} = (1 - \phi)(\rho c_p)_f + \phi(\rho c_p)_s, \quad (\rho \beta_T)_{nf} = (1 - \phi)(\rho \beta_T)_f + \phi(\rho \beta_T)_s, \\ (\rho \beta_C)_{nf} = (1 - \phi)(\rho \beta_C)_f + \phi(\rho \beta_C)_s. \end{aligned} \quad (2.9)$$

Non-dimensional forms corresponding to Eqs (2.1)-(2.5) are as follows

$$\frac{\partial U}{\partial X} + \frac{\partial V}{\partial Y} = 0, \quad (2.10)$$

$$\begin{aligned} \frac{\partial U}{\partial t} + U \frac{\partial U}{\partial X} + V \frac{\partial U}{\partial Y} = \frac{\rho_f}{\rho_{nf}} \left[\frac{I}{(I-\phi)^{2.5}} \frac{\partial^2 U}{\partial Y^2} - \frac{\sigma_{nf}}{\sigma_f} MU + \right. \\ \left. - Uk_p^2 + \frac{(\rho\beta_T)_{nf}}{(\rho\beta_T)_f} T \cos \infty + \frac{(\rho\beta_C)_{nf}}{(\rho\beta_C)_f} NC \cos \infty \right], \end{aligned} \quad (2.11)$$

$$\begin{aligned} \frac{\partial T}{\partial t} + U \frac{\partial T}{\partial X} + V \frac{\partial T}{\partial Y} = \frac{(\rho c_p)_f}{(\rho c_p)_{nf}} \left\{ \frac{K_{nf}}{k_f} \frac{I}{Pr} \frac{\partial^2 T}{\partial Y^2} + QT - \frac{RT}{Pr} + \right. \\ \left. + \varepsilon \left[\frac{\sigma_{nf}}{\sigma_f} MU^2 + \frac{I}{(I-\phi)^{2.5}} \left(\frac{\partial U}{\partial Y} \right)^2 \right] \right\}, \end{aligned} \quad (2.12)$$

$$\left(\frac{\partial C}{\partial t} + U \frac{\partial C}{\partial X} + V \frac{\partial C}{\partial Y} \right) = \frac{I}{Sc} \frac{\partial^2 C}{\partial Y^2} - K_c C. \quad (2.13)$$

Appropriate dimensionless conditions are

$$t \leq 0: U = 0, V = 0, T = 0, C = 0 \text{ for all } X, Y,$$

$$t > 0: U = 0, V = 0, T = X^n, C = X^m \text{ at } Y = 0, \quad (2.14)$$

$$U \rightarrow 0, T \rightarrow 0, C \rightarrow 0, \text{ as } Y \rightarrow \infty.$$

The local and average Sherwood number, Nusselt number and skin-friction coefficient are

$$\begin{aligned} Sh_x = Gr_L^{1/4} \left(\frac{\partial C}{\partial Y} \right)_{Y=0}, \quad Nu_x = Gr_L^{1/4} \left(-\frac{k_{nf}}{k_f} \right) \left(\frac{\partial T}{\partial Y} \right)_{Y=0}, \\ \tau_x = Gr_L^{3/4} \frac{I}{(I-\phi)^{2.5}} \left(\frac{\partial u}{\partial Y} \right)_{Y=0}, \quad \bar{Sh} = Gr_L^{1/4} \int_0^l \left(\frac{\partial C}{\partial Y} \right)_{Y=0} dX, \\ \bar{Nu} = Gr_L^{1/4} \left(-\frac{k_{nf}}{k_f} \right) \int_0^l \left(\frac{\partial T}{\partial Y} \right)_{Y=0} dX, \quad \bar{\tau} = Gr_L^{3/4} \frac{I}{(I-\phi)^{2.5}} \int_0^l \left(\frac{\partial U}{\partial Y} \right)_{Y=0} dX. \end{aligned} \quad (2.15)$$

3. Numerical procedure

The non-linear coupled Eqs (2.10)-(2.13) are solved by the Crank-Nicolson method using Eq.(2.14) which is unconditionally stable and converges quickly. The region which has to be integrated comprises a

rectangle of dimension $X_{max}(=1)$ and $Y_{max}(=24)$. Here, $Y_{max} = Y_{\infty}$ lies exterior to the boundary layers of Eqs (2.2)-(2.4). After a few preliminary studies, the value of Y is fixed as 24 to satisfy the tolerance limit 10^{-5} viewing the previous and the current boundary conditions. The local truncation error is $O(\Delta t^2 + \Delta Y^2 + \Delta X) \rightarrow 0$ as $\Delta t, \Delta Y, \Delta X \rightarrow 0$. Here the convergence is based on the compatibility and stability of the above scheme.

4. Results and discussion

In order to survey the impact of distinct variables on fluid velocity, temperature and concentration field, $Pr = 6.2, Sc = 0.16, R = 0.5, E = 0.3, Kp = 0.5, M = 0.5, Kc = 0.2, Q = 0.2, \alpha = 30$ are considered as common values exclusive of the values given in the appropriate graphs.

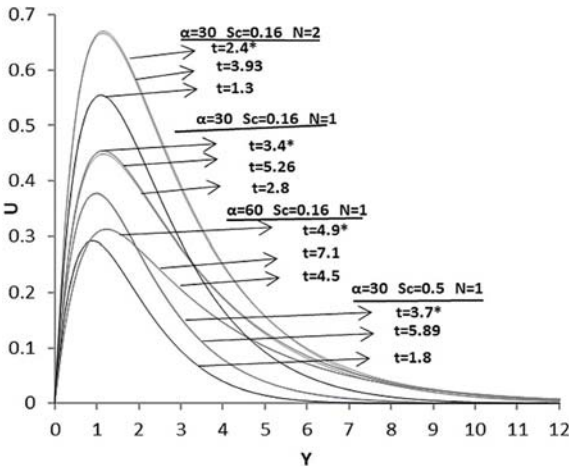


Fig.2. Velocity contour for various α, Sc and N (*steady state).

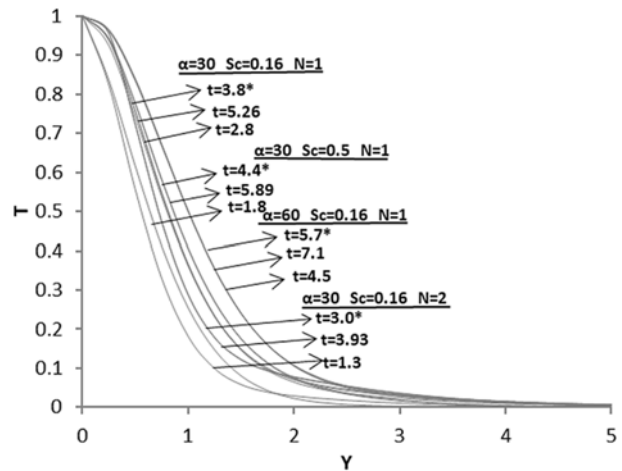


Fig.3. Temperature contour for various α, Sc and N (*steady state).

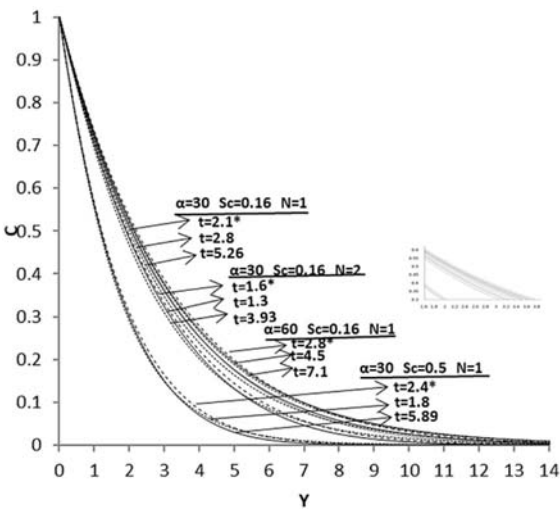


Fig.4. Concentration contour for various α, Sc and N (* steady state).

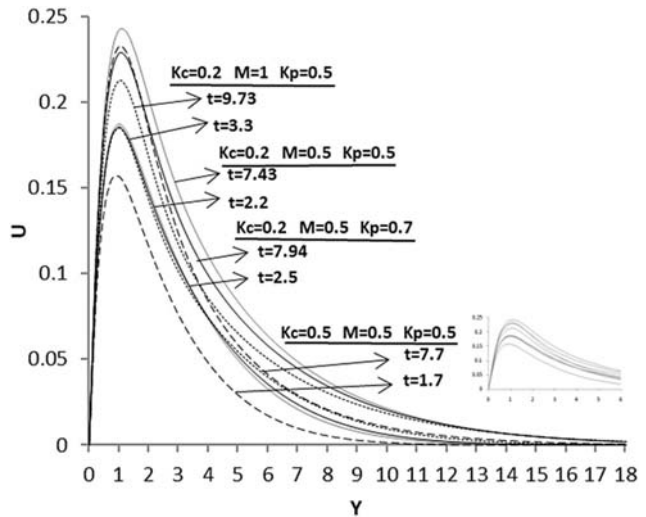


Fig.5. Velocity contour for various Kc, M and Kp .

Figure 2 reveals that with increasing the Schmidt number or inclination angle, the velocity of the nanofluid diminishes. An increment in the buoyancy ratio boosts the flow velocity and increases the boundary layer thickness. Figure 3 shows that the temperature field increases with increasing Schmidt number, but an increment in buoyancy ratio causes drops in the temperature field. It has been discovered that when the angle of inclination of the plate rises, the temperature field increases. Furthermore, the concentration field will be reduced, when the Schmidt number or buoyancy ratio proliferates. It is also worth noting that as α grows, the concentration field increases, as shown in Fig.4.

From Fig.5, it has been found that the velocity field of the copper water nanofluid increases as the value of the magnetic parameter falls. The transverse electromagnetic field creates a resistive force known as the electromagnetic force, which slows the fluid flow and reduces velocity. When we increase the permeability value, the fluid will flow freely through it, hence the velocity increases. Because of the loss of energy in species particles, velocity falls as the Kc value rises. Figure 6 shows how the temperature field rises as the value of M increases. With increasing permeability or chemical reaction parameter values, the temperature drops. Figure 7 shows that the concentration field increases and decreases the flow, respectively, as the magnetic field or permeability parameter increases, and with the growing Kc value, the concentration field declines.

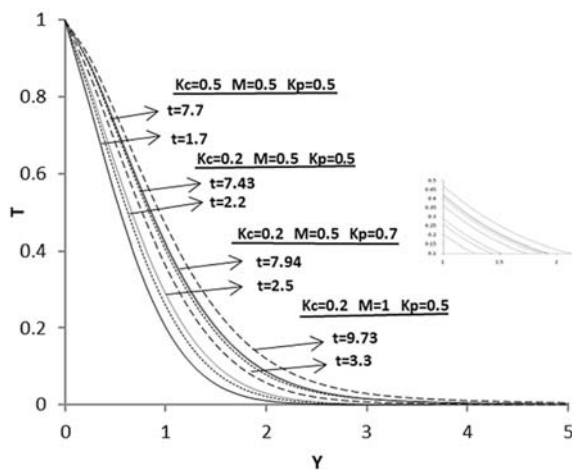


Fig.6. Temperature contour for various Kc , M and Kp .

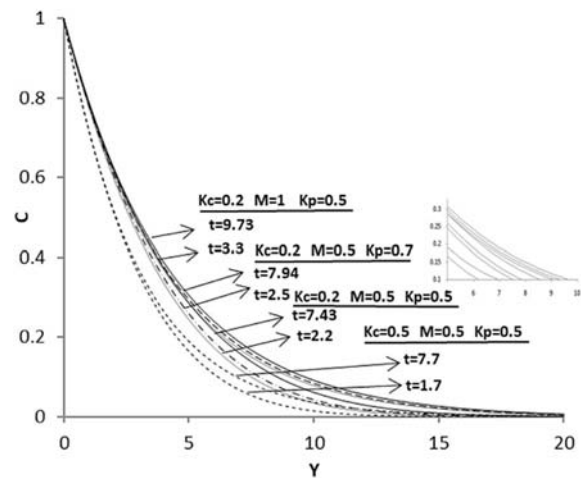


Fig.7. Concentration contour for various Kc , M and Kp .

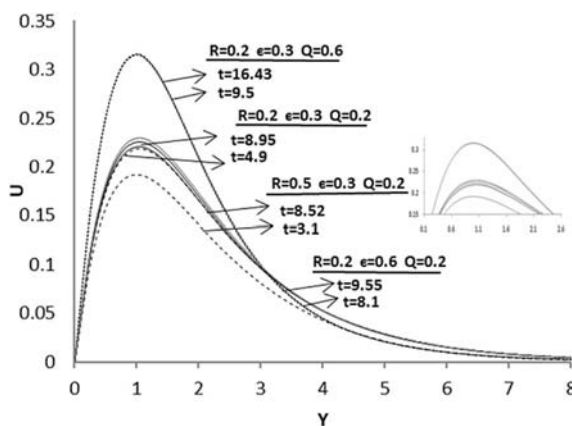


Fig.8. Velocity contour for various R , ϵ and Q .

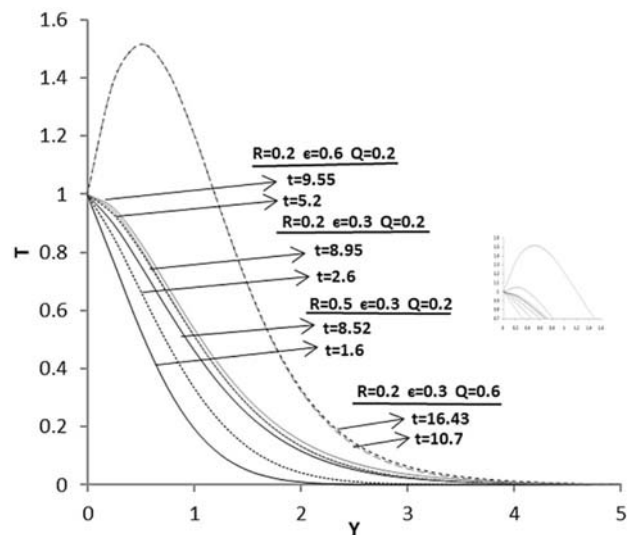


Fig.9. Temperature contour for various R , ϵ and Q .

Figure 8 demonstrates that when the heat source parameter is increased, velocity rises. It is noticeable that velocity decreases and delays the flow rate as R increases. It is observed that an increment in viscous dissipative heat leads to the proliferation of the velocity field. Here, increases in Q implied an increase in the temperature field. An increment in radiation R from 2.0 to 5.0 decreases the temperature field. Also, there will be a reduction in the temperature field as viscous dissipative heat is improved, as plotted in Figure 9. Figure 10 demonstrates that the concentration distribution declines gradually as Q increases. The value of R increases as the concentration field rises, but concentration of the fluid decreases as dissipative heat increases.

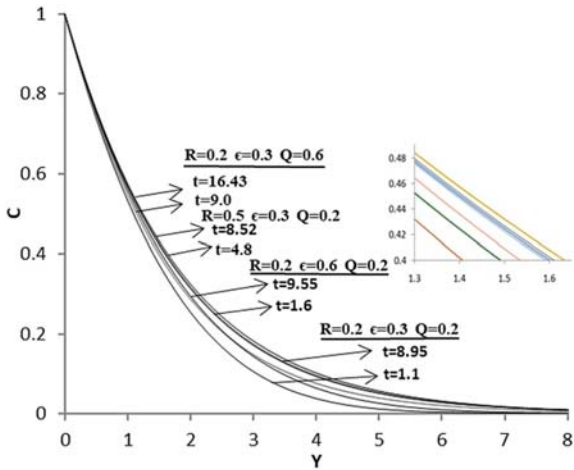


Fig.10. Concentration contour for various R , ϵ and Q .

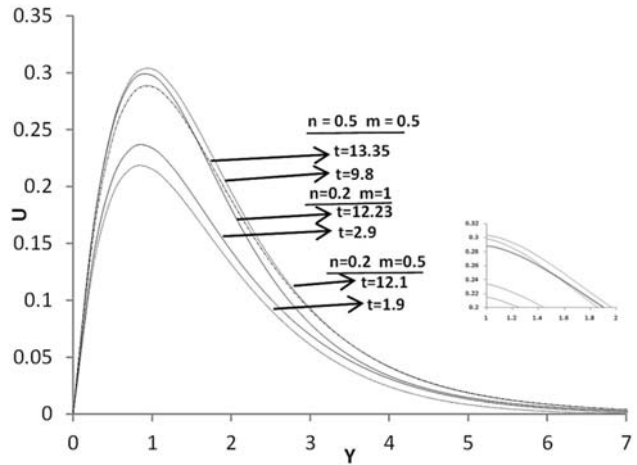


Fig.11. Velocity contour for various n and m .

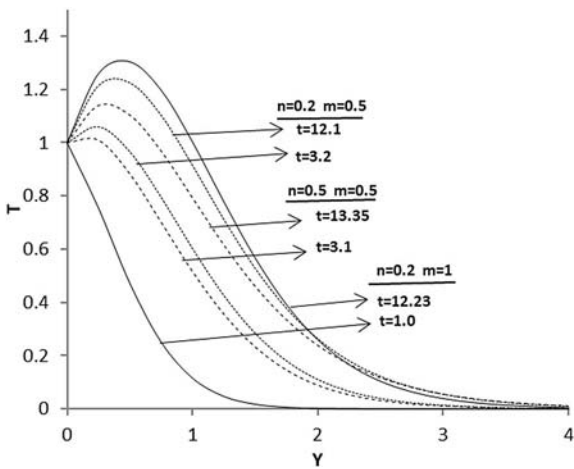


Fig.12. Temperature contour for various n and m .

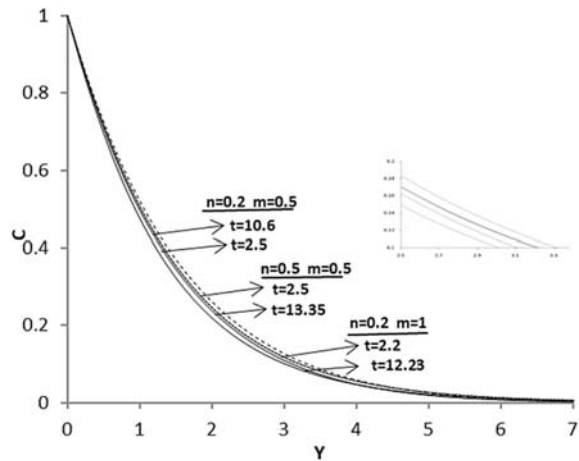


Fig.13. Concentration contour for various n and m .

As time increases, velocity rises till the temporal maximum is attained, after which velocity declines moderately. As n and m increase, the velocity fields decrease and increase respectively, as shown in Fig.11. The rate of drop of temperature in the direction of the heat flow through the plate close to the leading edge decreases as n increases, which means the driving force along the plate reduces with the increasing value of n . Also, it is observed that the dimensionless temperature increases for an increasing value of m , as depicted in Fig.12. The concentration profile rises with increasing exponent n value, and there will be a reduction in the concentration field for the higher m value, which is observed in Fig.13.

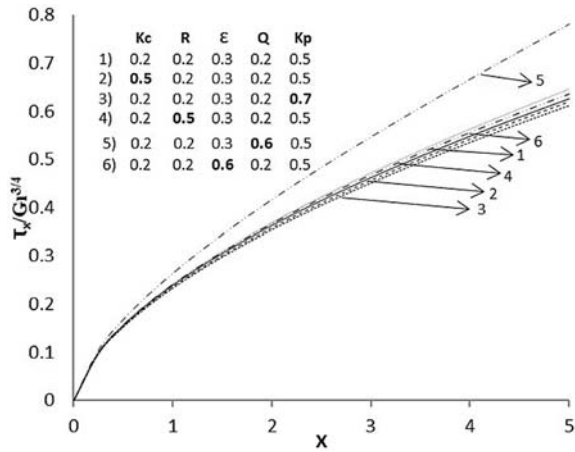


Fig.14. Local skin friction of Cu water nanofluid.

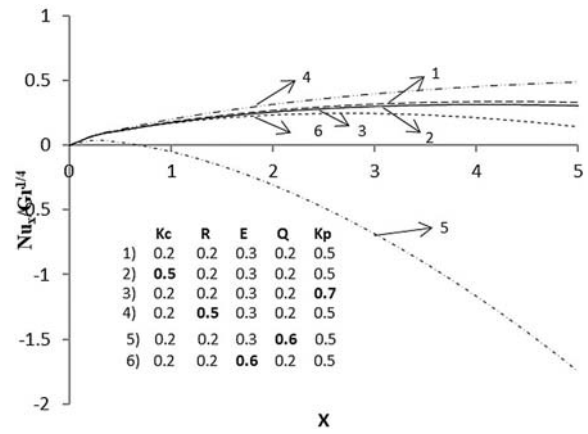


Fig.15. Local Nusselt number of Cu water nanofluid.

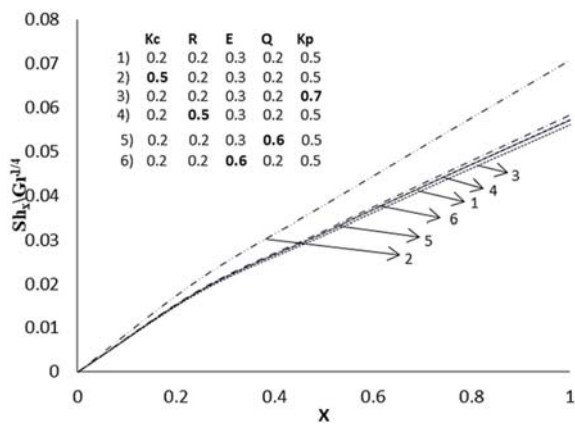


Fig.16. Local Sherwood number of Cu water nanofluid.

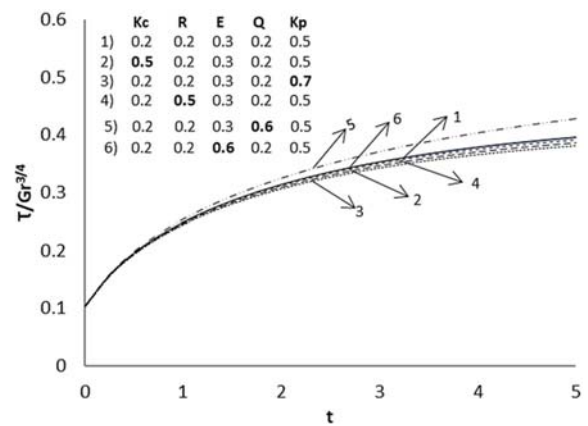


Fig.17. Average skin friction of Cu water nanofluid.

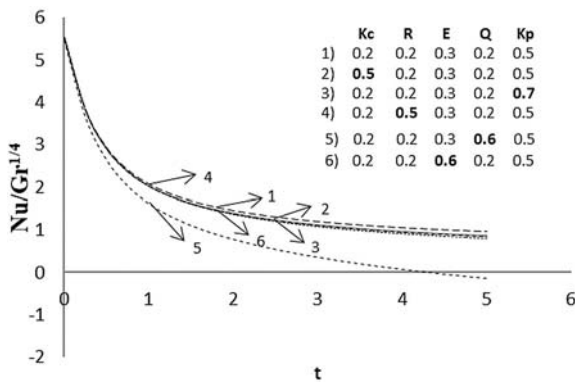


Fig.18. Average Nusselt number of Cu water nanofluid.

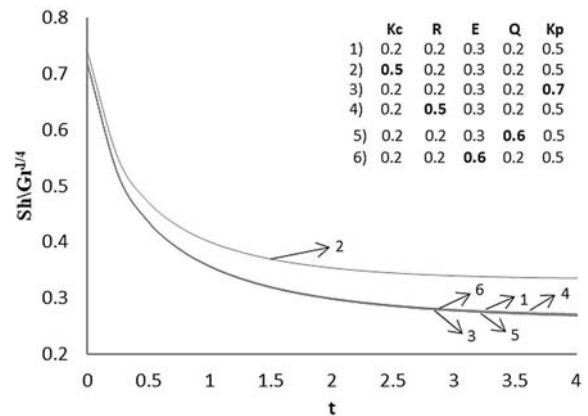


Fig.19. Average shear stress of Cu water nanofluid.

From Fig.14, it has been found that the local skin friction declines as the porous medium or chemical reaction or radiation parameter increases all through the transient period. We note that an increase in viscous dissipative heat and heat source parameters causes an increment in the average skin friction. The same results

are observed for the average skin friction in Fig.17. Figure 15 illustrates that an increase in radiation increases the local Nusselt number more than any other parameter mentioned in the graph. An increment in heat source parameters, chemical reaction, and porous medium decreases the local Nusselt number. Here, the negative value shows that the plate exerts a drag force on the nanofluid and a similar movement for the average Nusselt number is illustrated in Fig.18. The local Sherwood number proliferates as the chemical reaction value rises when compared to any other parameter mentioned in Fig.16. It is evident that the local Sherwood number increases with the decreasing value of porosity. The average Sherwood number behaviour is similar to that of the local Sherwood number concerning the mentioned parameters, whose graphical explanation is given in Fig.19.

4. Conclusion

An MHD free convective flow of copper water nanofluid past a semi-infinite plate inclined vertically at α with varying surface temperature as well as concentration in a porous medium was studied. An effective implicit finite difference technique was implemented to solve the dimensionless equations. The impacts of different factors were discussed through graphs.

1. The velocity field increases as the buoyancy ratio increases, while the temperature decreases as N increases.
2. An increase in Sc or Kc causes a decrease in the concentration and velocity fields.
3. Velocity and temperature fields are enhanced when the porosity is increased.
4. As the radiation parameter is increased, the velocity and temperature fields decrease.
5. The shear stress decreases with the decreasing value of the porosity or Kc .
6. The local Nusselt number rises as Q increases.

Acknowledgements

The authors are highly grateful to the reviewers for their valuable comments and suggestions on improving the quality of work. Also, the authors would like to thank the Department of Mathematics, Dr Ambedkar Govt Arts College, Chennai 600039, Tamil Nadu, INDIA and the Department of Mathematics, Bharathi Women's College, Chennai 600108, Tamil Nadu, INDIA for their continuous support.

Nomenclature

| | |
|--------------|--|
| B_0 | – applied magnetic field |
| C_w | – concentration of the fluid near the plate |
| $(c_p)_{nf}$ | – specific heat capacity of the nanofluid |
| g | – acceleration due to gravity |
| k'_p | – dimensioned permeability of the porous medium. |
| k'_c | – dimensioned chemical reaction parameter |
| k_{nf} | – thermal conductivity of the nanofluid |
| M | – magnetic field parameter |
| N | – buoyancy ratio parameter |
| Nu_x | – local Nusselt number |
| Pr | – Prandtl number |
| Q | – heat generation term |
| q_r | – radiative heat term |

- R – radiation parameter
 Sc – Schmidt number
 Sh_x – local Sherwood number
 T_w – temperature of the fluid near the plate
 u, v – velocity components in the coordinate system
 ϕ – solid volume fraction
 ρ_{nf} – density of the nanofluid
 μ_{nf} – dynamic viscosity of the nanofluid
 α – inclination parameter
 ν_f – kinematic viscosity of the base fluid
 σ_{nf} – electrical conductivity of the nanofluid
 τ_x – local skin friction coefficient
 $(\beta_T)_{nf}, (\beta_C)_{nf}$ – coefficients of thermal and concentration expansions, respectively

References

- [1] Chien-Hsin Chen (2004): *Combined heat and mass transfer in MHD free convection from a vertical surface with Ohmic heating and viscous dissipation.*– Int. J. Engng. Sci., vol.42, pp.699-713.
- [2] Palani G. and Kwang Yong Kim (2010): *Viscous dissipation effects on heat transfer in flow over an inclined plate.*– J. Appl. Mech. Tech Phys., vol.51, No.2, pp. 241-248.
- [3] Vasu B., Ramachandra Prasad V. and Bhaskar Reddy N. (2011): *Radiation and mass transfer effects on transient free convection flow of a dissipative fluid past semi-infinite vertical plate with uniform heat and mass flux.*– J. Appl. Fluid Mech., vol.4, No.1, pp.15-26.
- [4] Subhas Abel M., Kulkarni Anant Kumar and Ravikumara R. (2011): *MHD flow, and heat transfer with effects of buoyancy, viscous and joules dissipation over a nonlinear vertical stretching porous sheet with partial slip.*– Engng., vol.3, pp.285-291.
- [5] RamReddy Ch., Murthy P.V.S.N., Chamkha A.J. and Rashad A.M (2013): *Influence of viscous dissipation on free convection in a non-Darcy porous medium saturated with nanofluid in the presence of magnetic field.*– The Open Transport Pheno. J., vol.5, pp.20-29.
- [6] Ganesan P., Suganthi R.K. and Loganathan P. (2013): *Viscous and Ohmic heating effects in doubly stratified free convective flow over vertical plate with radiation and chemical reaction.*– Appl. Math. Mech. Engng., vol.34, No.2, pp.139-152.
- [7] Srikanth V.P.N., Srinivas G. and Reddy B.R.K. (2013): *MHD convective heat transfer of a nanofluid flow past an inclined permeable plate with heat source and radiation.*– Int. J. Phys. and Math Sci., vol.3, No.1, pp.89-95.
- [8] Dulal Pal and Gopinath Mandal (2015): *Mixed convection-radiation on stagnation-point flow of nanofluids over a stretching/shrinking sheet in a porous medium with heat generation and viscous dissipation.*– J. Petroleum Sci. Engng., vol.126, pp.16-25.
- [9] Hemalatha K., Krishna Keerthi A. and Sambasiva Rao G. (2014): *Flow and heat transfer analysis of a nanofluid along a vertical flat plate in presence of thermal radiation using similarity transformation method.*– IOSR J. Maths., vol.10, pp.41-48.
- [10] Meraj Mustafa, Ammar Mushtaq, Tasawar Hayat and Bashir Ahmad (2014): *Nonlinear radiation heat transfer effects in the natural convective boundary layer flow of nanofluid past a vertical plate: a numerical study.*– Plos One, vol.9, No.9. doi:10.1371/journal.pone.0103946.
- [11] Mohsen Sheikholeslami, Shirley Abelman and Davood Domiri Ganji (2014): *Numerical simulation of MHD nanofluid flow and heat transfer considering viscous dissipation.*– Int. J. Heat and Mass Transfer., vol.79, pp.212-222.

- [12] Gangaa B., Mohamed YusuffAnsarib S., Vishnu Ganeshc N. and Abdul Hakeem A.K.(2015):*MHD radiative boundary layer flow of nanofluid past a vertical plate with internal heat generation/absorption, viscous and Ohmic dissipation effects.*– J. of the Nigerian Math. Soc., vol. 34, pp.181-194.
- [13] Bhaskar Reddy N. Poornima T. and Sreenivasul P. (2015):*Internal heat generation and viscous dissipation effects on nanofluids over a moving vertical plate with convective boundary condition.*– Proc. ICFM Int. Con. on Frontiers in Mathematics, pp.123-129.
- [14] Loganathan P. and Sivapoornapriya C. (2016):*Ohmic heating and viscous dissipation effects over a vertical plate in the presence of porous medium.*– J. Appl. Fluid Mech., vol.9, No.1, pp.225-232.
- [15] Veeresh C., Varma S.V.K., Rushi Kumar B. and Vijaya Kumar A.G.(2016): *AG Heat and Mass Transfer in MHD mixed convection flow on a moving inclined porous plate.*– Int. J. Engng Res. in Africa., vol.20, pp.144-160.
- [16] Kumaresan E., Vijaya Kumarand A.G. and RushiKumar (2017): *An exact solution on unsteady MHD free convection chemically reacting silver nanofluid flow past an exponentially accelerated vertical plate through porous medium.*– IOP Conf. Ser. Materials Sci. Engng., vol.263, doi:10.1088/1757-899X/263/6/062018.
- [17] Prakash D., Suriyakumar P. and Rushi Kumar B. (2018):*Influence of viscous and Ohmic heating on MHD flow of nanofluid over an inclined nonlinear stretching sheet embedded in a porous medium.*– Int. J. Mech. Engng and Tech., vol 9, No.8, pp. 992-1001.
- [18] Sidda Reddy K., Chandra Reddy P. and Raju G.S.S. (2018): *Thermal diffusion and Joule heating effects on MHD radiating fluid embedded in porous medium.*– In.J. Res. Engng Application and Management., vol.4, No.4. pp.206-212.
- [19]Srinivasa A.H. and Ajay C.K.(2021):*Viscous dissipation, internal heat generation (absorption) effects on free convection flow about a vertical flat plate with an applied magnetic field.*– Int. J. Sci. Res. in Mathematical and Statistical Sci., vol.8, No.1, pp.27-31.

Received: May 3, 2022

Revised: July 22, 2022